Using human genetics to develop strategies to increase erythropoietic output from genome-edited hematopoietic stem and progenitor cells

Sofia E. Luna[1,2]*, Joab Camarena[1,2]*, Jessica P. Hampton[1,2], Kiran R. Majeti[1,2], Carsten T. Charlesworth[1,2], Eric Soupene[3], Sridhar Selvaraj[1,2], Kun Jia[4,5], Vivien A. Sheehan[6], M. Kyle Cromer[4,5,7]†, & Matthew H. Porteus[1,2]†

[1]Department of Pediatrics, Stanford University, Stanford, CA.

[2]Institute for Stem Cell Biology and Regenerative Medicine, Stanford University Stanford, CA.

[3]Department of Pediatrics, University of California, San Francisco, Oakland, CA.

[4]Department of Surgery, University of California, San Francisco, San Francisco, CA.

[5]Eli & Edythe Broad Center for Regeneration Medicine, University of California, San Francisco, San Francisco, CA, USA.

[6]Aflac Cancer Center and Blood Disorders, Department of Pediatrics, Emory University School of Medicine, Atlanta, GA.

[7]Department of Bioengineering & Therapeutic Sciences, University of California, San Francisco, San Francisco, CA, USA.

*Contributed equally

†Correspondence: kyle.cromer@ucsf.edu, mporteus@stanford.edu

Abstract

Human genetic polymorphisms result in a diversity of phenotypes. Some sequences are pathologic and lead to monogenic diseases, while others may confer beneficial traits. Genome editing is a powerful tool to recreate genotypes found in the population, including the ability to correct pathologic mutations. One of the best characterized naturally occurring mutations causing congenital erythrocytosis arises from a truncation in the erythropoietin receptor (tEPOR) which can result in non-pathogenic hyper-production of red blood cells (RBCs). Using the precision of CRISPR/Cas9 genome editing, we have recreated tEPOR and studied the effect of variations of the genotype on RBC development. We then combined tEPOR with a correction strategy developed for β-thalassemia and demonstrated that coupling the two genome editing events gave RBCs a significant selective advantage. This demonstrates the potential of combining human genetics with the precision of genome editing to enable safer and more effective genome editing therapies for patients with serious genetic diseases.

41 **Main**

42 Many of the initial applications of clinical genome editing have aimed to correct or
43 compensate for disease-causing mutations of monogenic diseases. However, human
44 genetic variation is more nuanced than monogenic diseases, as there are variants that
45 appear to confer positive health benefits as well. Examples are people that have bi-allelic
46 deletions in *CCR5* causing resistance to HIV infection, a variety of polymorphisms
47 causing upregulation of fetal hemoglobin, and mutations in *PCSK9* causing low
48 cholesterol levels[1–3]. It is important, however, to broadly assess variations that occur in
49 only small numbers of people for both their potential risks as well as for their potential
50 benefits.

51 Congenital erythrocytosis (CE) is a rare phenotype in which people have higher
52 than normal levels of red blood cells and consequently elevated hemoglobin. While there
53 are multiple genetic variants that can lead to this condition, perhaps the best
54 characterized genotype was first identified in the family of a Finnish Olympic gold medal-
55 winning cross-country skier who was found to have levels of hemoglobin >50% higher
56 than normal[4]. This was attributed to truncations in the erythropoietin receptor (tEPOR)
57 that eliminate elements of the intracellular inhibitory domain to erythropoietin (EPO)
58 signaling[4,5]. This domain contains binding sites for SHP1 which normally leads to
59 downregulation of EPO-dependent JAK2/STAT5 signaling (Extended Data Figure 1a).
60 Further studies have shown that tEPOR does not create a constitutively active EPOR
61 signaling cascade, but rather imparts hypersensitivity to EPO[5,6]. As a consequence, these
62 kindreds with tEPOR typically present with abnormally low levels of EPO, indicating a new
63 homeostasis is attained to prevent CE from becoming pathogenic. There have been

64 reports of thrombotic and hemorrhagic events likely due to erythrocytosis but many of
65 these have a benign clinical course[7]. More importantly, families with CE have not shown
66 an increased predisposition to cancer, demonstrating that this is not a pre-malignant
67 genetic condition[8].

68 While prior studies, including those by the Smithies group and Tisdale group, have
69 investigated the effects of viral-mediated delivery and expression of *tEPOR*[9–11], random
70 insertion into the genomes of billions of hematopoietic stem and progenitor cells (HSPCs)
71 in the context of bone marrow transplant presents a serious safety concern, and has
72 resulted in a “Black Box” warning in the United States for lovotibeglogene autotemcel, a
73 lentiviral gene therapy drug approved for sickle cell disease[12]. In addition, such instances
74 of viral-mediated delivery require expression of *tEPOR* using a non-native, exogenous
75 promoter, which departs from native *EPOR* regulation and has the potential for
76 unintended consequences such as pathogenic polycythemia. Nonetheless, viral-
77 mediated expression studies provide a proof-of-concept that demonstrates that *tEPOR*
78 expression can lend a selective advantage to transduced cells and provide a foundation
79 for the utilization of more advanced genome engineering modalities.

80 Genome editing is a powerful method that enables the precise changing of
81 nucleotides in the DNA of a cell. There are multiple genome-editing strategies including
82 nuclease-based insertion/deletion (indel) formation, base editing, and prime editing, but
83 the most versatile approach to genome-editing is homology-directed repair (HDR). In
84 HDR, a nuclease-induced double-strand break (DSB) is repaired using a donor template.
85 The natural donor template for HDR is the sister chromatid and the natural repair pathway
86 is homologous recombination. By providing a donor template that resembles a sister

87 chromatid with large homology arms flanking the intended cut site, the homologous
88 recombination machinery can use this “substitute” sister chromatid to repair the DSB.
89 HDR editing is the most flexible because it can create single nucleotide changes,
90 precisely insert large gene cassettes, and even swap out large genomic regions for other
91 gene sequences[13–16]. We utilize all of these applications of HDR in this work, including
92 direct creation of the naturally occurring variant found in a human kindred.

93 One of the challenges in hematopoietic stem cell gene therapy is to achieve
94 sufficient engraftment of the genetically engineered cells to have a beneficial clinical effect
95 without increasing risk. To make this possible, effort is exerted to maximize editing
96 frequencies in HSPCs[17–19]. Even if clinically relevant editing frequencies are achieved,
97 high-morbidity chemo-therapeutic regimens are currently required to create niche space
98 in the bone marrow (BM) for these edited HSPCs, which can create toxicities, including
99 oncogenic risk[20–22]. In this work, we aimed to give edited cells a selective advantage such
100 that low levels of engraftment might still result in a clinical benefit, perhaps enabling less
101 toxic conditioning, through use of genome editing to recreate the CE phenotype by
102 engineering tEPOR into HSPCs in different ways. We find that when tEPOR is engineered
103 into human HSPCs using genome-editing, there is a significant selective advantage to
104 the derived red blood cells (RBCs). We then show that this selective advantage can be
105 coupled to a therapeutic gene edit to give the cells with the therapeutic edit a selective
106 advantage in RBC development, without affecting the stem and progenitor cells. In this
107 way, we demonstrate the power of combining human genetics with precision genome
108 editing to potentially enable safer and more effective genome editing therapies for
109 patients with serious genetic diseases, particularly those of red blood cells.

110

111 **Results**

112 **Cas9-guided EPOR truncation in HSPCs enhances erythroid proliferation**

113 Truncating mutations in the *EPOR* gene that cause clinically benign congenital
114 erythrocytosis[4,8] provide a potentially safe avenue to increase erythropoietic output from
115 genome-edited HSPCs. In this study we designed Cas9 single-guide RNAs (sgRNAs)[17]
116 (termed *EPOR*-sg1 and *EPOR*-sg2) that overlap the location of the originally identified
117 nonsense mutation, *EPOR* c.1316G>A (p.W439X) ("Mäntyranta variant")[4]. (Figure 1a,
118 Extended Data Figure 2a). Our hypothesis was that targeting this site in exon 8 with Cas9
119 would create a spectrum of indels, a subset of which would result in a frameshift of the
120 reading frame and yield premature downstream stop codons in the *EPOR* gene.

121 To test this hypothesis, we pre-complexed each sgRNA with high-fidelity Cas9
122 protein[23] and delivered these ribonucleoprotein (RNP) complexes to human $CD34^+$
123 HSPCs. At 2-3 days post-editing, we transferred cells into culture media that promotes
124 erythroid differentiation over the course of two weeks[24] (Figure 1a). To determine whether
125 edited HSPCs have a proliferative advantage compared to unedited cells, we harvested
126 genomic DNA at days 0, 4, 7, 11, and 14 of RBC differentiation. We then quantified indel
127 frequency by PCR amplification followed by Sanger sequencing and decomposition
128 analysis using TIDE[25]. In the absence of a selective advantage or disadvantage, percent
129 edited alleles in cells at the beginning and end of RBC differentiation will be roughly
130 equivalent—which is what we observe for the editing frequency of the *HBB* sgRNA used
131 for correction of sickle cell disease. However, we observe that the editing frequency of
132 *EPOR*-targeting sgRNAs increases significantly over the course of erythroid

133 differentiation, to a greater extent in *EPOR*-sg1 than *EPOR*-sg2 (Figure 1b, Extended
134 Data Figure 2b) (P=0.0016 for *EPOR*-sg1 from day 0 to day 14). Additionally, we show
135 that the increase in indels for both *EPOR*-sg1 and *EPOR*-sg2 are predominantly driven
136 by indels that yield downstream stop codons (Extended Data Figure 2c-d, Extended Data
137 Figure 3a-b). This indicates that edited cells, particularly those with premature stop
138 codons, are outcompeting unedited cells because of the EPO hypersensitivity of tEPOR-
139 expressing cells in culture[5,6].

140 Because not all indels created by the sgRNAs cause truncations in *EPOR*, we
141 speculated that we could increase this proliferative effect by using HDR to insert a stop
142 codon at the exact location of the original variant (c.1316G>A). To accomplish this, we
143 designed an AAV6 repair template vector that introduces a stop codon into *EPOR* at the
144 439th amino acid (W439X) followed by a BGH-polyA tail to terminate transcription. We
145 also included a downstream GFP marker driven by the constitutive human UbC promoter
146 to ensure that each GFP^+ allele harbors the intended *EPOR*-truncating mutation. The
147 entire integration cassette was flanked by 950-base pair homology arms that
148 corresponded to the genomic DNA immediately upstream and downstream of the
149 intended Cas9 cut site created by the more effective *EPOR*-sg1 (Figure 1c). To determine
150 whether this editing strategy was also able to drive enrichment of genome-edited RBCs,
151 we complexed *EPOR*-sg1 with Cas9 protein and delivered this by electroporation to
152 human $CD34^+$ HSPCs followed by transduction with AAV6 DNA repair template. Two to
153 three days post-editing we either maintained cells in HSPC media or began erythroid
154 differentiation with 3 U/mL of EPO (+EPO), as has been previously described[14], or with 0
155 U/mL of EPO (-EPO) in order to determine whether *tEPOR*-expressing cells retain EPO

156 sensitivity or became EPO independent during their differentiation. At day 14 of erythroid
157 differentiation, we stained for established RBC markers[14] and analyzed cells using flow
158 cytometry. We observed no differentiation when cells were kept in HSPC media and
159 efficient RBC differentiation in all treatments with EPO. In the edited conditions in the
160 absence of EPO, we observed moderate differentiation which may indicate the
161 hypersensitivity of tEPOR-expressing cells to trace amounts of EPO in the media, as has
162 been previously observed[4] (Figure 1d). By analyzing GFP^+ cells over the course of RBC
163 differentiation, in the *EPOR*^{W439X}-edited conditions we observed a significant increase in
164 the frequency of edited cells in only the +EPO conditions (P=0.0006 comparing day 0 to
165 day 14) (Figure 1e). At the end of differentiation, by quantifying both GFP^+ cells and
166 frequency of indel formation, we estimate that almost all the RBCs are derived from cells
167 with a truncated EPOR due to either an indel or a UbC-GFP knock-in event (Extended
168 Data Figure 4a). In addition to the competitive advantage that *tEPOR* expression gives to
169 edited cells over the course of RBC differentiation, we also observed increased RBC
170 production in both *EPOR*-sg1 and *EPOR*-sg1 + UbC-GFP-BGH conditions compared to
171 Mock control in the +EPO condition (average 1.45×10^3 total fold increase in mock edited
172 cells versus 4.71×10^3 in *EPOR*-sg1 + UbC-GFP-BGH over the 14-day RBC
173 differentiation) (Figure 1f). These increased cell counts were not observed in the -EPO
174 condition or when cells were maintained in HSPC media, indicating an EPO-driven
175 increase in erythroid proliferation in cells expressing *tEPOR* (Extended Data Figure 4b).
176 We also assessed whether a gradient of EPO concentrations (0 U/mL – 20 U/mL) over
177 the course of RBC differentiation yielded varying degrees of enrichment of edited cells
178 (Extended Data Figure 5a). On day 14, when compared to 0 U/mL EPO, we found minimal

179 differences in GFP$^+$ cells in the 1, 3, and 20 U/mL conditions and only a minor reduction
180 in GFP$^+$ cells in the 0.3 U/mL EPO condition (Extended Data Figure 5b-c), indicating that
181 even low levels of EPO is sufficient to impart a selective advantage to edited cells
182 consistent with prior work on the natural variants[5,6]. We also observed comparable levels
183 of RBC differentiation at all concentrations except 0 U/mL EPO (Extended Data Figure
184 5d).

185 In terms of the safety of this editing strategy, we show that introduction of these
186 *EPOR* indels yields RBCs with production of both fetal and adult hemoglobin tetramers
187 following hemoglobin tetramer high-performance liquid chromatography (HPLC)
188 (Extended Data Figure 6a). We also found similar colony number and lineage distribution
189 from CD34$^+$ HSPCs plated into wells containing methylcellulose media either with or
190 without EPO that were scored for colony-formation ability after 14 days (Extended Data
191 Figure 6b). As expected, there was a marked decrease in the ability to form BFU-E
192 colonies in the absence of EPO even if the cells contained the tEPOR. These data
193 reinforce the idea that truncation of EPOR does not alter the lineage bias of HSPCs, but
194 rather has an effect only after commitment to the erythroid lineage. Additionally, although
195 transient delivery of high-fidelity Cas9 has been shown to be highly specific to the on-
196 target site[26], we also evaluated potential off-target effects of the *EPOR*-sg1-RNP complex
197 in HSPCs. We found that 94% (73/78) of candidate off-target sites with scores previously
198 shown to be most informative for identifying sites with potential off-target activity[27] resided
199 in intergenic or intronic regions of the genome (Extended Data Figure 7a-b). We further
200 interrogated potential off-target activity at the five sites that resided in exonic or UTR

201 regions of genes (Extended Data Figure 7c) and found no evidence of off-target activity
202 in *EPOR*-sg1-edited cells when compared to mock edited cells (Extended Data 7d-e).
203

204 **Integration of *tEPOR* cDNA at safe-harbor locus recapitulates the proliferative**
205 **effect**

206 Given the therapeutic utility of transgene integration at safe harbor sites[28], we
207 hypothesized that integration of a *tEPOR* cDNA at a safe harbor site may also enable
208 increased erythroid production from edited HSPCs while leaving the endogenous *EPOR*
209 locus intact. Given the fact that integration at the *CCR5* locus is an established method
210 for delivery of therapeutic transgenes in HSPCs[29], we developed a custom AAV6-
211 packaged DNA repair template that would facilitate integration of an exogenous human
212 UbC promoter driving expression of *tEPOR* cDNA followed by a T2A-YFP-BGH reporter
213 (Figure 2a). Given the strong, constitutive expression of the UbC promoter, this method
214 of insertion is expected to express *tEPOR* ubiquitously in all hematopoietic cell types,
215 regardless of lineage.

216 To test this strategy for *tEPOR* expression, we edited HSPCs with Cas9
217 complexed with an established sgRNA targeting exon 2 of *CCR5*[29] (*CCR5*-sg3),
218 immediately followed by transduction with our custom DNA repair template. We then
219 performed RBC differentiation post-editing and analyzed the kinetics of editing frequency,
220 YFP expression, and erythroid differentiation using droplet digital PCR (ddPCR) and flow
221 cytometry. As with endogenous *EPOR* truncation strategies, we observed more efficient
222 erythroid differentiation in all treatments with EPO compared to the minus EPO conditions
223 (Figure 2b). While flow cytometry confirmed the ubiquitous expression of YFP in edited

224 cells, regardless of presence of CD71 and GPA erythroid markers during differentiation
225 (Figure 2c), we did observe significant enrichment of YFP-expressing RBCs in the
226 presence of EPO ($P<0.0001$ when comparing day 0 to day 14 of RBC differentiation
227 (Figure 2d)). This enrichment was confirmed at the genomic level by ddPCR which
228 showed an increase in percent edited alleles when *tEPOR*-expressing cells were
229 subjected to erythroid differentiation, increasing by an average of 7.3-fold in the presence
230 of EPO, as well as enrichment to a limited degree enrichment in the -EPO condition
231 (Extended Data Figure 8a). With this editing strategy, we observed increased RBC
232 production in the CCR5-sg3 + *tEPOR* condition and no increase in proliferation of CCR5-
233 sg3 alone compared to mock control cells in the +EPO condition. We saw no increased
234 proliferation in the cells maintained in HSPC media or in the -EPO condition (Extended
235 Data Figure 8b). We then assessed if enrichment of edited cells differed along a gradient
236 of EPO levels during RBC differentiation and again found that there were minimal
237 differences in YFP^+ cells in the 1, 3, and 20 U/mL conditions and a minor decrease in the
238 0.3 U/mL EPO condition compared to 0 U/mL EPO (Extended Data Figure 8c-d). There
239 were comparable levels of RBC differentiation in all conditions except 0 U/mL EPO
240 (Extended Data Figure 8e).

241 We once again observed that edited and unedited cells had no noticeable
242 difference in lineage commitment or colony-forming ability following a colony-forming unit
243 assay (Extended Data Figure 9a). In addition, we analyzed RBCs post-differentiation
244 using hemoglobin tetramer HPLC and found that UbC-mediated expression of *tEPOR*
245 resulted in both HgbF and HgbA expression but a relative increase in HgbF expression
246 (Extended Data Figure 9b). These results indicate that expression of *tEPOR* from a safe

247 harbor site is an effective means of driving increased RBC production from genome-
248 edited HSPCs.
249
250 **Integration of *tEPOR* cDNA at *HBA1* demonstrates an erythroid-specific**
251 **proliferative effect**
252 While integration at a safe harbor locus effectively increased erythropoietic output from
253 edited HSPCs, there is the concern that constitutive expression in all cell types could
254 disrupt stem-ness or lead to other unintended effects. As an alternative, we can introduce
255 promoter-less transgenes into endogenous genes in order for the integration cassette to
256 be regulated by endogenous expression machinery. For instance, in prior work we
257 designed a genome editing strategy to fully replace the *HBA1* gene with an *HBB*
258 transgene in order to correct β-thalassemia[14]. We found that because α-globin is
259 produced by duplicate genes, *HBA1* may serve as a safe harbor site to deliver custom
260 payloads with strong erythroid-specific expression.
261 We therefore hypothesized that integration of the *tEPOR* cDNA at the *HBA1* locus
262 could further enhance production of edited RBCs while avoiding potential complications
263 with ubiquitous transgene expression because of the specificity of expression of *HBA1* in
264 the RBC lineage. To test this hypothesis, we designed a custom integration cassette (also
265 packaged in AAV6) to use with an established sgRNA (*HBA1*-sg4) to introduce a
266 promoter-less *tEPOR* cDNA followed by a T2A-YFP reporter under expression of
267 endogenous *HBA1* regulatory machinery (Figure 2e). Following editing, we observed
268 efficient erythroid differentiation in all treatments with EPO and little to no differentiation
269 in the absence of EPO (Figure 2f). We found that this integration strategy indeed yielded

270 RBC-specific expression of YFP, which was only detectable as cells gained CD71 and
271 GPA erythroid markers (Figure 2g). Over the course of RBC differentiation, we observed
272 dramatic enrichment of YFP^+ cells exclusively in the +EPO condition (Figure 2h). While
273 we observed a mild degree of enrichment of edited alleles using ddPCR in the absence
274 of EPO, this effect was more pronounced in the presence of EPO, eliciting an average
275 4.4-fold increase in percentage of edited alleles over the course of RBC differentiation
276 (Extended Data Figure 10a). We again cultured edited cells in a gradient of EPO during
277 RBC differentiation and this time observed minimal differences in YFP^+ cell enrichment in
278 all conditions containing EPO (Extended Data Figure 10b-c). There were also comparable
279 levels of RBC differentiation in all conditions except 0 U/mL EPO (Extended Data Figure
280 10d).

281 Once again, we found that cells edited with *tEPOR* at *HBA1* demonstrated similar
282 colony-forming ability as mock edited cells (Extended Data Figure 11a). Additionally, we
283 found that *tEPOR*-expressing cells produce ratios of human hemoglobin that are similar
284 to unedited RBCs (Extended Data Figure 11b).

285

286 **Combined *HBB-tEPOR* bicistronic cassettes simultaneously correct β-thalassemia**
287 **and increase production of edited RBCs**

288 Because the above results demonstrate that *tEPOR* expression yields increased RBC
289 production from edited HSPCs, we then sought to couple this selective advantage with a
290 therapeutic gene edit. We chose to combine tEPOR with our prior β-thalassemia
291 correction approach to simultaneously correct the disease and increase production of
292 clinically meaningful RBCs from these corrected HSPCs. One way this can be

293 accomplished is by creating a bicistronic cassette that links expression of the therapeutic
294 full-length *HBB* transgene with a *tEPOR* cDNA. Prior studies have found that the type of
295 linker domain used can have a great bearing on transgene expression and protein
296 function—particularly when function is dependent on formation of protein complexes, as
297 is the case with the globin genes[14]. Therefore, we designed and tested a variety of AAV6
298 repair template vectors linking the two genes using standard T2A peptides, optimized T2A
299 peptides with Furin cleavage sites[30] (referred to as "FuT2A"), internal ribosome entry sites
300 (referred to as "IRES"), as well by driving *tEPOR* expression from a separate exogenous
301 promoter—human PGK1 (referred to as "PGK"). To evaluate the different vectors, we
302 edited healthy donor HSPCs as previously described at *HBA1* using the bicistronic AAV6
303 repair templates and evaluated their ability to differentiate and enrich for edited RBCs
304 over the course of erythroid differentiation (Figure 3a). While efficient RBC differentiation
305 was achieved in all editing conditions (Figure 3b), we found that all four bicistronic
306 cassettes drove >2-fold enrichment of edited alleles (range: 2.1-fold to 3.5-fold) (P=0.003
307 for PGK-tEPOR, P=0.0055 for T2A-tEPOR, P=0.0259 for F2A-tEPOR, and P=0.0003 for
308 IRES-tEPOR when comparing day 0 to day 14) (Figure 3c-d). We note that allele targeting
309 frequencies of 60% translates into >80% of the cells having at least one allele targeted
310 (cell targeting frequency) and thus would not expect to see much more enrichment than
311 we observed.

312 To ensure this strategy was also effective in patient-derived cells, we tested these
313 bicistronic vectors in HSPCs derived from sickle cell disease (SCD) patients, this time
314 comparing them to a therapeutic full-length *HBB* transgene[14]. All of the constructs are
315 knocked-in to the *HBA1* locus without disrupting the endogenous *HBB* locus expressing

316 HgbS. We found that vectors did not disrupt erythroid differentiation when compared to
317 mock edited cells in the same donor, although their ability to differentiate was likely
318 impacted by the variable quality of the frozen patient samples (Extended Data Figure
319 12a). Again, we observed >2-fold enrichment of edited alleles for all four bicistronic
320 vectors (range: 2.0-fold to 3.1-fold), but no change in editing frequency for the original β-
321 thalassemia correction vector (P=0.0061 for PGK-tEPOR, P=0.011 for T2A-tEPOR,
322 P=0.0016 for Fu2A-tEPOR, P=0.0153 for IRES-tEPOR when comparing day 0 to day 14)
323 (Figure 3e-f). We estimate that at the end of the differentiation almost all of the cells have
324 at least one allele with the HBB-tEPOR knock-in and thus no biologic drive for further
325 enrichment. When we analyzed differentiated RBCs for hemoglobin tetramers by HPLC,
326 we found that the 2A vectors showed almost no HgbA expression (consistent with what
327 has been seen previously in which addition of a 2A can disrupt HBB protein function[31]).
328 In contrast, we found that PGK-tEPOR and IRES-tEPOR vectors showed an improvement
329 in HgbA production relative to the *HBB*-only edited cells (Extended Data Figure 12b).
330 There was no change in the HgbF expression in these samples.
331

332 **Multiplexed genome editing to introduce *tEPOR* and *HBB* leads to robust increase**
333 **in *β-globin* mRNA in edited RBCs**

334 In lieu of coupling the *tEPOR* cDNA and therapeutic edit at the same locus, an alternative
335 strategy would be to multiplex two editing events at different loci to simultaneously
336 truncate the endogenous *EPOR* and introduce the original β-thalassemia correction
337 vector at *HBA1*. This may have the additional advantage that the endogenous *EPOR*
338 truncation will more reliably recapitulate congenital erythrocytosis. We hypothesized that

339 we could simultaneously deliver Cas9 separately pre-complexed with *EPOR*-truncating
340 *EPOR*-sg1 and *HBA1*-sg4 sgRNA and then transduce HSPCs with both the β-
341 thalassemia correction vector as well as the W439X *EPOR*-targeting vector. Because
342 homology arms of each vector are specific for each site—*HBB* for the *HBA1* locus and
343 W439X for the *EPOR* locus—integration for each vector will occur only at the intended
344 locus. This strategy may allow simultaneous correction of β-thalassemia and increased
345 erythropoietic output from corrected HSPCs. For this to be maximally effective, the two
346 editing events must be present in the same cell. Therefore, during editing we used a DNA-
347 PKcs inhibitor to increase the frequency of template integration at each locus[32,33].
348 Following editing, we determined whether this multiplexed editing strategy increases the
349 frequency of corrected RBCs over the course of erythroid differentiation.

350 To model the clinical setting where both edited and unedited HSPCs would occupy
351 the patient's bone marrow, we introduced unedited cells at various concentrations at the
352 start of erythroid differentiation (Figure 4a). Importantly, none of the multiplexed
353 conditions disrupted erythroid differentiation compared to single-edited *HBB* or mock
354 conditions (Figure 4b). In all of the multiplexed conditions, we observed an increase in
355 the frequency of corrected alleles over the course of RBC differentiation (P=0.0332 for
356 *HBB*+*tEPOR* 100%, P=0.0086 for *HBB*+*tEPOR* 30%, P=0.0122 for *HBB*+*tEPOR* 10%
357 when comparing day 0 to day 14) (Figure 4c). In fact, in both the 30% and 10%
358 multiplexed conditions, we achieved a higher frequency of edited alleles by the conclusion
359 of erythroid differentiation compared to single-edited conditions with unedited cells
360 introduced at an equivalent concentration (P=0.0113 for *HBB* versus *HBB*+*tEPOR* 30%
361 at day 14 and P=0.008 for *HBB* versus *HBB*+*tEPOR* 10% at day 14) (Figure 4d). We

362 confirmed truncation at the *EPOR* locus measured by GFP^+ cells at day 14 of RBC
363 differentiation (Extended Data Figure 13a). We also observed a corresponding increase
364 in *HBB* mRNA expression from the *HBA1* locus in the 30% and 10% multiplexed edited
365 conditions on day 14 of RBC differentiation compared to single-edited conditions (Figure
366 4e), indicating an improved ability for multiplexed editing to increase therapeutic potential
367 of this β-thalassemia correction strategy. When we measured the colony-forming ability
368 of the edited cells and found that differentiation into the various lineages was similar
369 between mock cells and cells edited with *HBB* alone or *HBB*+*tEPOR*, although we did
370 observe a decrease in total colonies produced in both edited conditions as would be
371 expected from the increased amount of AAV used to target two loci[34,35] (Extended Data
372 Figure 13b-c).
373

374 **Discussion**

375 While insights from clinical genetics have typically implicated novel genes and
376 pathways in disease, here we sought to use human genetics to develop novel strategies
377 to *treat* disease. We used the precision of genome editing to capitalize on a previously
378 characterized disorder called congenital erythrocytosis, which leads to EPO
379 hypersensitivity and hyperproduction of erythrocytes, without causing pathology[4]. As
380 demonstrated previously with variants identified in human genetics, such as those found
381 in *CCR5*, *PCSK9*, and the gamma-globin promoter region, we hypothesized that we could
382 use CRISPR to introduce this natural *EPOR* variant (*tEPOR*) to increase erythropoietic
383 output from edited HSPCs. Prior work has highlighted the challenge of achieving long-
384 term correction of disease following delivery of gene therapy or genome editing correction

385 strategies[2,36,37]. While many efforts are underway to improve editing and engraftment
386 frequencies, we hypothesized that we could develop a strategy to increase production of
387 the clinically relevant cell type—the red blood cell—from edited HSPCs. If successful,
388 then lower editing and engraftment frequencies could yield sufficient production of RBCs
389 to achieve therapeutic benefit, and thus be curative for patients. Uchida *et al*. have shown
390 that introducing the *tEPOR* variant using lentiviral delivery enhanced the efficacy of
391 shRNA knockdown of *BCL11A* in upregulating HgbF, confirming the beneficial function of
392 this variant[9]. However, our work deploys the precision of genome editing to generate
393 tEPOR which may have broad utility across a spectrum of blood disorders.

394 We explored multiple genome-editing strategies to create the *tEPOR* variant, either
395 through truncation of the endogenous *EPOR* gene or integration of a *tEPOR* cDNA at
396 safe harbor loci. We found that HSPCs expressing *tEPOR* consistently demonstrated
397 increased erythropoiesis but otherwise normal, EPO-dependent production of
398 hemoglobin. In order to increase RBC production of genome-edited HSPCs in the context
399 of disease correction, we combined the *tEPOR* cassette with a previously described β-
400 thalassemia strategy in which the *HBB* gene replaces the *HBA1* gene using homology-
401 directed repair-based genome editing[14]. This allowed us to simultaneously introduce an
402 *HBB* transgene to restore normal hemoglobin production and to increase erythropoietic
403 output from edited HSPCs. To demonstrate the flexibility of the various *tEPOR*-
404 introduction strategies, we also developed an alternative multiplexed, site-specific
405 genome editing strategy to pair the original β-thalassemia correction strategy with
406 introduction of the *EPOR* truncation at the endogenous locus. Both strategies led to
407 enrichment of genome-edited RBCs over the course of erythroid differentiation compared

408 to the traditional β-thalassemia correction strategy. Because we found the effects to be
409 EPO-dependent, it is possible the selective advantage *in vivo* may be even more
410 pronounced because patients suffering from the hemoglobinopathies display elevated
411 EPO levels due to their severe anemia[38].

412 In terms of safety, the strategy to use CRISPR to introduce natural variants has
413 the benefit of having been already "tested" *in vivo* in humans. However, it must be noted
414 that several of the genome editing strategies introduce *tEPOR* under non-native
415 regulation which could alter the normal function of tEPOR. In considering this possibility,
416 we note while every cell in patients with CE harbor an *EPOR* truncation, therapeutic
417 deployment of the genome editing strategy will result in the introduction of *tEPOR* in only
418 a subset of HSPCs resident in the BM. Therefore, any aberrant effects of non-native
419 *tEPOR* expression (e.g., bias away from lymphoid or other cell types) are unlikely to lead
420 to cytopenia given the large number of unedited HSPCs remaining in the bone marrow
421 post-transplant. Furthermore, by increasing erythropoietic output from edited HSPCs, we
422 believe this work could enable the reduction or elimination of high-morbidity myeloablation
423 regimens that are currently required to attain therapeutic levels of edited HSPCs.
424 Expression of *tEPOR* could therefore be integrated into any treatment for blood disorders
425 that involve transplantation of HSPCs. For example, even in an allogeneic hematopoietic
426 stem cell transplant for red blood cell disorders, a truncation in the natural *EPOR* could
427 be created using indel-based genome editing to give the derived transplanted erythroid
428 progenitors a selective advantage. This strategy could thereby enable less toxic
429 myeloablative conditioning to be effectively utilized where mixed chimerism might be the
430 result.

431 Taken together, these results demonstrate the power of combining knowledge
432 from human genetics with the precision of CRISPR genome editing technology to
433 introduce clinically meaningful variants. As human genome sequencing becomes more
434 commonplace and clinically routine[39,40], it is likely that a greater number of variants of
435 unknown significance will be discovered and characterized. We therefore believe that the
436 strategy defined in this work—using CRISPR to introduce natural human variants—may
437 be deployed to amplify the therapeutic potential of current and future cell therapies.

438 **Methods**

439 **AAV6 vector design, production, and purification.** Adeno-associated virus, serotype
440 6 (AAV6) vector plasmids were cloned into the pAAV-MCS plasmid (Agilent
441 Technologies, Santa Clara, CA, USA), comprised of inverted terminal repeats (ITRs)
442 derived from AAV2. Gibson Assembly Mastermix (New England Biolabs, Ipswich, MA,
443 USA) was used for the creation of all DNA repair vectors as per manufacturer's
444 instructions. AAV6 vector was produced and purified with little variation from previously
445 described processes[41]. 293T cells (Life Technologies, Carlsbad, CA, USA) were seeded
446 in five 15 cm^2 dishes with 13-15×10^6 cells per plate 24 hours pre-transfection. Then, each
447 dish was transfected with a standard polyethylenimine (PEI) transfection of 6 µg ITR-
448 containing plasmid and 22 µg pDGM6 (gift from David Russell, University of Washington,
449 Seattle, WA, USA), which holds the AAV6 cap, AAV2 rep, and Ad5 helper genes.
450 Following a 48-72h incubation, cells were harvested and vectors were purified using the
451 AAVpro purification kit (cat.: 6666; Takara Bio, Kusatsu, Shiga, Japan) as per
452 manufacturer's instructions and stored at -80 °C until further use. AAV6 vectors were
453 titered using ddPCR to measure the number of vector genomes as previously described[42].
454

455 ***In vitro* culture of CD34⁺ HSPCs.** Human CD34⁺ HSPCs were cultured in conditions as
456 previously described[13,43–46]. CD34⁺ HSPCs were isolated from cord blood (provided by
457 Stanford Binns Program for Cord Blood Research) or sourced from Plerixafor- and/or G-
458 CSF-mobilized peripheral blood (AllCells, Alameda, CA, USA and STEMCELL
459 Technologies, Vancouver, Canada). Frozen Plerixafor- and/or G-CSF-mobilized
460 peripheral blood of patients with sickle cell disease were provided by Dr. Vivien Sheehan,

461 Emory University. $CD34^+$ HSPCs were cultured at 1×10^5–5×10^5 cells/mL in StemSpan
462 Serum-Free Expansion Medium II (STEMCELL Technologies, Vancouver, Canada) or
463 Good Manufacturing Practice Stem Cell Growth Medium (SCGM, CellGenix, Freiburg,
464 Germany) supplemented with a human cytokine (PeproTech, Rocky Hill, NJ, USA)
465 cocktail: stem cell factor (100 ng/mL), thrombopoietin (100 ng/mL), Fms-like tyrosine
466 kinase 3 ligand (100 ng/ml), interleukin 6 (100 ng/mL), streptomycin (20 mg/mL), and
467 penicillin (20 U/mL), and 35 nM of UM171 (cat.: A89505; APExBIO, Houston, TX, USA).
468 The cell incubator conditions were 37°C, 5% CO_2, and 5% O_2.
469
470 **Electroporation-aided transduction of cells.** The synthetic chemically modified
471 sgRNAs used to edit $CD34^+$ HSPCs were purchased from Synthego (Redwood City, CA,
472 USA) or TriLink Biotechnologies (San Diego, CA, USA) and were purified by HPLC.
473 These modifications are comprised of 2′-O-methyl-3′-phosphorothioate at the three
474 terminal nucleotides of the 5′ and 3′ ends described previously[17]. The target sequence for
475 the sgRNAs were as follows:
476
477 *EPOR* sgRNA (*EPOR*-sg1)
478 5′-AGCTCAGGGCACAGTGTCCA-3′
479
480 *EPOR* sgRNA (*EPOR*-sg2)
481 5′-GCTCCCAGCTCTTGCGTCCA-3′
482
483 *CCR5* sgRNA (*CCR5*-sg3)

484 5′-GCAGCATAGTGAGCCCAGAA-3′

485

486 *HBA1* sgRNA (*HBA1*-sg4)

487 5′-GGCAAGAAGCATGGCCACCG-3′

488

489 The HiFi Cas9 protein was purchased from Integrated DNA Technologies (IDT)
490 (Coralville, Iowa, USA) or Aldevron (Fargo, ND, USA). Preceding electroporation, RNPs
491 were complexed at a Cas9:sgRNA molar ratio of 1:2.5 at 25°C for 10-20 min. Next, $CD34^+$
492 cells were resuspended in P3 buffer (Lonza, Basel, Switzerland) with complexed RNPs
493 and subsequently electroporated using the Lonza 4D Nucleofector and 4D-Nucleofector
494 X Unit (program DZ-100). Electroporated cells were then plated at 1×10^5-5×10^5 cells/mL
495 in the previously described cytokine-supplemented media. Immediately following
496 electroporation, AAV6 was dispensed onto cells at 2.5×10^3-5×10^3 vector genomes/cell
497 based on titers determined by ddPCR. For multiplex editing experiments, in addition to
498 the steps described above, cells were incubated with 0.5 μM of a DNA-PKcs inhibitor,
499 AZD7648 (cat.: S8843; Selleck Chemicals, Houston, TX) for 24 hours, as previously
500 described[32,33].

501

502 **Allelic modification analysis using ddPCR.** Edited HSPCs were harvested within 2-3
503 days post-electroporation and at each media change throughout erythrocyte
504 differentiation and then analyzed for modification frequencies of the alleles of interest. To
505 quantify editing frequencies, we created custom ddPCR primers and probes to quantify
506 HDR alleles (using in-out PCR and probe corresponding to the expected integration

507 event) compared to an established genomic DNA reference (REF) at the *CCRL2* locus[14].
508 QuickExtract DNA extraction solution (Biosearch Technologies, Hoddesdon, UK, cat.:
509 QE09050) was used to collect genomic DNA (gDNA) input, which was then digested
510 using BamHI-HF or HindIII-HF as per the manufacturer's instructions (New England
511 Biolabs, Ipswich, MA, USA). The percentage of targeted alleles within a cell population
512 was measured with a Bio-Rad QX200 ddPCR machine and QuantaSoft software (v.1.7;
513 Bio-Rad, Hercules, CA, USA) using the following reaction mixture: 1-4 µL gDNA input, 10
514 µL of ddPCR SuperMix for Probes (no dUTP) (Bio-Rad), primer/probes (1:3.6 ratio; IDT),
515 and volume up to 20 µL with H_2O. ddPCR droplets were then generated following the
516 manufacturer's instructions (Bio-Rad): 20 µL of ddPCR reaction, 70 µL of droplet
517 generation oil, and 40 µL of droplet sample. Thermocycler (Bio-Rad) settings were as
518 follows: 98°C (10 min), 94°C (30 s), 55.7-60°C (30 s), 72°C (2 min), return to step 2 × 40–
519 50 cycles, and 98°C (10 min). Analysis of droplet samples was then performed using the
520 QX200 Droplet Digital PCR System (Bio-Rad). We next divided the copies/µL for HDR
521 (%): HDR (FAM) / REF (HEX). The following primers and probes were used in the ddPCR
522 reaction:
523
524 *CCR5 (for tEPOR-YFP construct)*
525 Forward Primer (FP): 5'-GGGAGGATTGGGAAGACA-3'
526 Reverse Primer (RP): 5'-AGGTGTTCAGGAGAAGGACA-3'
527 Probe: 5'-6-FAM/AGCAGGCATGCTGGGGATGCGGTGG/3IABkFQ-3'
528
529 *HBA1 (for tEPOR-YFP construct)*

530 FP: 5’-AGTCCAAGCTGAGCAAAGA-3’

531 RP: 5’-ATCACAAACGCAGGCAGAG-3’

532 Probe: 5’-CGAGAAGCGCGATCACATGGTCCTGC-3’

533

534 *HBA1 (for HBB construct and tEPOR-HBB constructs)*

535 FP: 5’-GTGGCTGGTGTGGCTAATG-3’

536 RP: 5’-CAGAAAGCCAGCCAGTTCTT-3’

537 Probe: 5’-6-FAM/CCTGGCCCACAAGTATCACT/3IABkFQ-3’

538

539 *HBA1 (for HBB-tEPOR constructs)*

540 FP: 5’-TCTGCTGCCAGCTTTGAGTA-3’

541 RP: 5’-GCTGGAGTGGGACTTCTCTG-3’

542 Probe: 5’-6-FAM/ACTATCCTGGACCCCAGCTC/3IABkFQ-3’

543

544 *CCRL2 (reference)*

545 FP: 5’- GCTGTATGAATCCAGGTCC-3’,

546 RP: 5’- CCTCCTGGCTGAGAAAAAG -3’

547 Probe: 5’- HEX/TGTTTCCTC/ZEN/CAGGATAAGGCAGCTGT/3IABkFQ -3’

548

549 **Indel analysis using TIDE software.** Within 2-4 days post-electroporation, HSPCs were

550 harvested with QuickExtract DNA extraction solution (Biosearch Technologies, cat.:

551 QE09050) to collect gDNA. The following primer sequences were used to amplify the

552 respective cut site at the *EPOR* locus*:*

553 FP: 5'-CAGCTGTGGCTGTACCAGAA-3'

554 RP: 5'-CAGCCTGGTGTCCTAAGAGC-3'

555 Sanger sequencing of respective samples was then used as input for indel frequency
556 analysis relative to a mock, unedited sample using TIDE as previously described[25].

557

558 ***In vitro* differentiation of CD34$^+$ HSPCs into erythrocytes.** Following editing, HSPCs
559 derived from healthy or sickle cell disease patients were cultured 2-3 days as described
560 above. Subsequently, a 14-day *in vitro* differentiation was performed in supplemented
561 SFEMII medium as previously described[24,47]. SFEMII base medium was supplemented
562 with 100 U/mL penicillin–streptomycin, 10 ng/mL SCF (PeproTech, Rocky Hill, NJ, USA),
563 1 ng/mL IL-3 (PeproTech, Rocky Hill, NJ, USA), 3 U/mL EPO (eBiosciences, San Diego,
564 CA, USA), 200 µg/mL transferrin (Sigma-Aldrich, St. Louis, MO, USA), 3% human serum
565 (heat-inactivated from Sigma-Aldrich, St. Louis, MO, USA or Thermo Fisher Scientific,
566 Waltham, MA, USA), 2% human plasma (isolated from umbilical cord blood provided by
567 Stanford Binns Cord Blood Program), 10 µg/mL insulin (Sigma-Aldrich, St. Louis, MO,
568 USA), and 3 U/mL heparin (Sigma-Aldrich, St. Louis, MO, USA). Cells were cultured in
569 the first phase of medium for seven days at 1×10^5 cells/mL. In the second phase of
570 medium, day 7-10, cells were maintained at 1×10^5 cells/mL, and IL-3 was removed from
571 the culture. In the third phase of medium, day 11-14, cells were cultured at 1×10^6 cells/mL,
572 with a transferrin increase to 1 mg/mL.

573

574 **Immunophenotyping of differentiated erythrocytes.** Differentiated erythrocytes were
575 analyzed by flow cytometry on day 14 for erythrocyte lineage-specific markers using a

576 FACS Aria II (BD Biosciences, San Jose, CA, USA). Edited and unedited cells were
577 analyzed using the following antibodies: hCD45-V450 (HI30; BD Biosciences, San Jose,
578 CA, USA), CD34-APC (561; BioLegend, San Diego, CA, USA), CD71-PE-Cy7 (OKT9;
579 Affymetrix, Santa Clara, CA, USA), and CD235a-PE (GPA) (GA-R2; BD Biosciences). In
580 addition to cell-specific markers, cells were also stained with Ghost Dye Red 780 (Tonbo
581 Biosciences, San Diego, CA, USA) to measure viability.
582
583 **Hemoglobin tetramer analysis.** Frozen pellets of approximately 1×10^6 cells *in vitro*-
584 differentiated erythrocytes were thawed and lysed in 30 µL of RIPA buffer with 1x Halt™
585 Protease Inhibitor Cocktail (Thermo Fisher Scientific, Waltham, MA, USA) for 5 minutes
586 on ice. The mixture was vigorously vortexed and cell debris were removed by
587 centrifugation at 13,000 RPM for 10 minutes at 4°C. HPLC analysis of hemoglobins in
588 their native form was performed on a cation-exchange PolyCAT A column (35 × 4.6 mm^2,
589 3 µm, 1,500 Å) (PolyLC Inc., Columbia, MD, USA) using a Perkin-Elmer Flexar HPLC
590 system (Perkin-Elmer, Waltham, MA, USA) at room temperature and detection at 415 nm.
591 Mobile phase A consisted of 20 mM Bis-tris and 2 mM KCN at pH 6.94, adjusted with HCl.
592 Mobile phase B consisted of 20 mM Bis-tris, 2 mM KCN, and 200 mM NaCl at pH 6.55.
593 Hemolysate was diluted in buffer A prior to injection of 20 µL onto the column with 8%
594 buffer B and eluted at a flow rate of 2 mL/min with a gradient made to 40% B in 6 min,
595 increased to 100% B in 1.5 min, and return to 8% B in 1 min and equilibrated for 3.5 min.
596 Quantification of the area under the curve of the peaks was performed with TotalChrom
597 software (Perkin-Elmer, Waltham, MA, USA) and raw values were exported to GraphPad
598 Prism 9 for plotting and further analysis.

599

600 **mRNA analysis.** Following differentiation of HSPCs into erythrocytes, cells were
601 harvested, and RNA was extracted using the RNeasy Plus Mini Kit (Qiagen, Hilden,
602 Germany). Subsequently, complementary DNA was made from approximately 100 ng of
603 RNA using the iScript Reverse Transcription Supermix for quantitative PCR with reverse
604 transcription (Bio-Rad, Hercules, CA, USA). Expression levels of β-globin transgene and
605 α-globin mRNA were quantified with a Bio-Rad QX200 ddPCR machine and QuantaSoft
606 software (v.1.7; Bio-Rad, Hercules, CA, USA) using the following primers and 6-FAM/
607 ZEN/IBFQ-labeled hydrolysis probes, purchased as custom-designed PrimeTime qPCR
608 Assays from IDT:
609 *HBB and HBB-tEPOR into HBA1:*
610 FP: 5'-GGTCCCCACAGACTCAGAGA-3'
611 RP: 5'-CAGCATCAGGAGTGGACAGA
612 Probe: 5'-6-FAM/AACCCACCATGGTGCATCTG/3IABkFQ -3'
613 To normalize for RNA input, levels of the RBC-specific reference gene GPA were
614 determined in each sample using the following primers and HEX/ZEN/IBFQ-labeled
615 hydrolysis probes, purchased as custom-designed PrimeTime qPCR Assays from IDT:
616 *GPA (reference):*
617 FP: 5′-ATATGCAGCCACTCCTAGAGCTC-3′
618 RP: 5′-CTGGTTCAGAGAAATGATGGGCA-3′
619 Probe: 5'- HEX/AGGAAACCGGAGAAAGGGTA/3IABkFQ -3'
620 ddPCR reactions were created using the respective primers and probes, and droplets
621 were generated as described above. Thermocycler (Bio-Rad; settings were as follows:

622 98°C (10 min), 94°C (30 s), 54°C (30 s), 72°C (30 s), return to step 2 × 50 cycles, and
623 98°C (10 min). Analysis of droplet samples was done using the QX200 Droplet Digital
624 PCR System (Bio-Rad). To determine relative expression levels, the numbers of *HBB*
625 transgene copies/mL were divided by the numbers of *GPA* copies/mL.
626
627 **Methylcellulose colony forming unit (CFU) assay.** 2-3 days post-electroporation
628 HSPCs were plated in SmartDish 6-well plates (cat.: 27370; STEMCELL Technologies,
629 Vancouver, Canada) containing MethoCult H4434 Classic or MethoCult H4434 Classic
630 without EPO (cat.: 04444; cat: 04544.; STEMCELL Technologies, Vancouver, Canada).
631 After 14 days, the wells were imaged using the STEMvision Hematopoietic Colony
632 Counter (STEMCELL Technologies, Vancouver, Canada). Colonies were counted and
633 scored to determine the number of BFU-E, CFU-E, CFU-GM, and CFU-GEMM colonies.
634
635 **Quantification of editing efficiency at evaluated off-target sites.** Potential sgRNA off-
636 target sites were predicted using the CRISPR Off-target Sites with Mismatches,
637 Insertions, and Deletions (COSMID) online tool[48]. Sites were ranked according to score
638 and duplicate predictions at the same location were removed. All sites with a score ≤5.5
639 were included in analysis and the 5 sites in exonic or UTR regions were further analyzed.
640 PCR amplification of these sites was performed using genomic DNA from mock-edited
641 and RNP-edited cells. The following primers were used with Illumina adapters (FP
642 adapter: 5'-ACACTCTTTCCCTACACGACGCTCTTCCGATCT-3', RP adapter: 5'-
643 GACTGGAGTTCAGACGTGTGCTCTTCCGATCT-3'):
644 *EPOR-OT1*

645 FP: 5’-GAGCGGGCTACAGAGCTAGA-3’

646 RP: 5’-TGGCAGAAAGTAAGGGGATG-3’

647

648 *EPOR-OT2*

649 FP: 5’-ACTTGTGGAGCCACAGTTTG-3’

650 RP: 5’-AATGCCCTTGAGATGAATGC-3’

651

652 *EPOR-OT3*

653 FP: 5’-TCACACACCCGTAGCCATAA-3’

654 RP: 5’-AGAATGCTCTTTGCAGTAGCC-3’

655

656 *EPOR-OT4*

657 FP: 5’-CTCAAAACTTCACCCAGGCT-3’

658 RP: 5’-GGTCTGTCATTGAATGCCTT-3’

659

660 *EPOR-OT5*

661 FP: 5’-CAACCCTGATGGGTCTGC-3’

662 RP: 5’-CCACAGCTGGCTGACCTT-3’

663 Following amplification, PCR products were purified by gel electrophoresis and
664 subsequent extraction using the GeneJet Gel Extraction Kit (Thermo Fisher Scientific,
665 Waltham, MA, cat.: FERK0692). Purified samples were submitted for library preparation
666 and sequencing by Amplicon-EZ NGS (Azenta Life Sciences, San Francisco, CA),
667 ensuring a yield of over 100,000 reads per sample. Amplicons, flanked by Illumina partial

adapter sequences, which encompassed the programmed double-strand breaks (DSBs) for CRISPR/Cas9, underwent sequencing using Illumina chemistry. FastQC (v0.11.8, http://www.bioinformatics.babraham.ac.uk/projects/fastqc/, default parameters) was employed to assess the quality of raw reads. Subsequently, paired-end reads were aligned to the specified off-target regions using CRISPResso2 (version 2.2.14, CRISPResso --fastq_r1 reads_r1.fastq.gz --fastq_r2 reads_r2.fastq.gz --amplicon_seq)[49].

Statistical analysis. GraphPad Prism 9 software was used for all statistical analysis.

Data availability. All data supporting the findings of this study are available within the paper and its Supplementary Information. High-throughput sequencing data generated for off-target analysis will be uploaded to the NCBI Sequence Read Archive submission.

681 **Acknowledgements**

682 The authors thank the following funding sources that made this work possible: American
683 Society of Hematology Junior Faculty Scholar Award to M.K.C.; Stanford Medical
684 Scholars Research Program, the American Society of Hematology Minority Medical
685 Student Award Program, and the Stanford Medical Scientist Training Program to S.E.L.;
686 American Society of Hematology Minority Medical Student Award Program to J.C. We
687 would also like to thank the Stanford Binns Program for Cord Blood Research for
688 providing $CD34^+$ HSPCs and the FACS Core Facility at the Stanford Institute of Stem Cell
689 Biology and Regenerative Medicine for access to FACS machines.

690

691 **Competing interests**

692 MHP is on the Board of Directors of Graphite Bio. M.H.P. serves on the scientific advisory
693 board of Allogene Tx and is an advisor to Versant Ventures. M.H.P., M.K.C., and J.C.
694 have equity in Graphite Bio. M.H.P. has equity in CRISPR Tx.

References

1. Hütter G, Nowak D, Mossner M, et al. Long-Term Control of HIV by CCR5 Delta32/Delta32 Stem-Cell Transplantation. *N Engl J Med*. 2009;360(7):692-698. doi:10.1056/NEJMoa0802905

2. Frangoul H, Altshuler D, Cappellini MD, et al. CRISPR-Cas9 Gene Editing for Sickle Cell Disease and β-Thalassemia. *N Engl J Med*. 2021;384(3):252-260. doi:10.1056/NEJMoa2031054

3. Fitzgerald K, White S, Borodovsky A, et al. A Highly Durable RNAi Therapeutic Inhibitor of PCSK9. *N Engl J Med*. 2017;376(1):41-51. doi:10.1056/NEJMoa1609243

4. de la Chapelle A, Träskelin AL, Juvonen E. Truncated erythropoietin receptor causes dominantly inherited benign human erythrocytosis. *Proc Natl Acad Sci U S A*. 1993;90(10):4495-4499.

5. Sokol L, Luhovy M, Guan Y, Prchal J, Semenza G, Prchal J. Primary familial polycythemia: a frameshift mutation in the erythropoietin receptor gene and increased sensitivity of erythroid progenitors to erythropoietin. *Blood*. 1995;86(1):15-22. doi:10.1182/blood.V86.1.15.bloodjournal86115

6. Juvonen E, Ikkala E, Fyhrquist F, Ruutu T. Autosomal dominant erythrocytosis caused by increased sensitivity to erythropoietin. *Blood*. 1991;78(11):3066-3069.

7. Huang LJ, Shen YM, Bulut GB. Advances in understanding the pathogenesis of primary familial and congenital polycythaemia. *Br J Haematol*. 2010;148(6):844-852. doi:10.1111/j.1365-2141.2009.08069.x

8. Arcasoy MO, Degar BA, Harris KW, Forget BG. Familial erythrocytosis associated with a short deletion in the erythropoietin receptor gene. *Blood*. 1997;89(12):4628-4635.

9. Uchida N, Ferrara F, Drysdale CM, et al. Sustained fetal hemoglobin induction in vivo is achieved by BCL11A interference and coexpressed truncated erythropoietin receptor. *Sci Transl Med*. 2021;13(591):eabb0411. doi:10.1126/scitranslmed.abb0411

10. Negre O, Fusil F, Colomb C, et al. Correction of murine β-thalassemia after minimal lentiviral gene transfer and homeostatic in vivo erythroid expansion. *Blood*. 2011;117(20):5321-5331. doi:10.1182/blood-2010-01-263582

11. Kirby SL, Cook DN, Walton W, Smithies O. Proliferation of multipotent hematopoietic cells controlled by a truncated erythropoietin receptor transgene. *Proc Natl Acad Sci U S A*. 1996;93(18):9402-9407.

729 12. Hacein-Bey-Abina S, Garrigue A, Wang GP, et al. Insertional oncogenesis in 4
730 patients after retrovirus-mediated gene therapy of SCID-X1. *J Clin Invest*.
731 2008;118(9):3132-3142. doi:10.1172/JCI35700

732 13. Dever DP, Bak RO, Reinisch A, et al. CRISPR/Cas9 β-globin gene targeting in
733 human haematopoietic stem cells. *Nature*. 2016;539(7629):384-389.
734 doi:10.1038/nature20134

735 14. Cromer MK, Camarena J, Martin RM, et al. Gene replacement of α-globin with β-
736 globin restores hemoglobin balance in β-thalassemia-derived hematopoietic stem
737 and progenitor cells. *Nat Med*. 2021;27(4):677-687. doi:10.1038/s41591-021-01284-
738 y

739 15. Vaidyanathan S, Salahudeen AA, Sellers ZM, et al. High-Efficiency, Selection-free
740 Gene Repair in Airway Stem Cells from Cystic Fibrosis Patients Rescues CFTR
741 Function in Differentiated Epithelia. *Cell Stem Cell*. 2020;26(2):161-171.e4.
742 doi:10.1016/j.stem.2019.11.002

743 16. Choi E, Koo T. CRISPR technologies for the treatment of Duchenne muscular
744 dystrophy. *Mol Ther*. 2021;29(11):3179-3191. doi:10.1016/j.ymthe.2021.04.002

745 17. Hendel A, Bak RO, Clark JT, et al. Chemically modified guide RNAs enhance
746 CRISPR-Cas genome editing in human primary cells. *Nat Biotechnol*.
747 2015;33(9):985-989. doi:10.1038/nbt.3290

748 18. Shin JJ, Schröder MS, Caiado F, et al. Controlled Cycling and Quiescence Enables
749 Efficient HDR in Engraftment-Enriched Adult Hematopoietic Stem and Progenitor
750 Cells. *Cell Rep*. 2020;32(9):108093. doi:10.1016/j.celrep.2020.108093

751 19. Transient Inhibition of 53BP1 Increases the Frequency of Targeted Integration in
752 Human Hematopoietic Stem and Progenitor Cells. doi:10.21203/rs.3.rs-2621625/v1

753 20. Chakraborty NG, Bilgrami S, Maness LJ, et al. Myeloablative chemotherapy with
754 autologous peripheral blood stem cell transplantation for metastatic breast cancer:
755 immunologic consequences affecting clinical outcome. *Bone Marrow Transplant*.
756 1999;24(8):837-843. doi:10.1038/sj.bmt.1701999

757 21. Bhatia S. Long-term health impacts of hematopoietic stem cell transplantation inform
758 recommendations for follow-up. *Expert Rev Hematol*. 2011;4(4):437-454.
759 doi:10.1586/ehm.11.39

760 22. Inamoto Y, Shah N, Savani B, et al. Secondary solid cancer screening following
761 hematopoietic cell transplantation. *Bone Marrow Transplant*. 2015;50(8):1013-1023.
762 doi:10.1038/bmt.2015.63

763 23. Vakulskas CA, Dever DP, Rettig GR, et al. A high-fidelity Cas9 mutant delivered as
764 a ribonucleoprotein complex enables efficient gene editing in human hematopoietic

765 stem and progenitor cells. *Nat Med*. 2018;24(8):1216-1224. doi:10.1038/s41591-
766 018-0137-0

767 24. Dulmovits BM, Appiah-Kubi AO, Papoin J, et al. Pomalidomide reverses γ-globin
768 silencing through the transcriptional reprogramming of adult hematopoietic
769 progenitors. *Blood*. 2016;127(11):1481-1492. doi:10.1182/blood-2015-09-667923

770 25. Brinkman EK, Chen T, Amendola M, van Steensel B. Easy quantitative assessment
771 of genome editing by sequence trace decomposition. *Nucleic Acids Res*.
772 2014;42(22):e168. doi:10.1093/nar/gku936

773 26. Cromer MK, Barsan VV, Jaeger E, et al. Ultra-deep sequencing validates safety of
774 CRISPR/Cas9 genome editing in human hematopoietic stem and progenitor cells.
775 *Nat Commun*. 2022;13(1):4724. doi:10.1038/s41467-022-32233-z

776 27. Cromer MK, Majeti KR, Rettig GR, et al. Comparative analysis of CRISPR off-target
777 discovery tools following ex vivo editing of CD34+ hematopoietic stem and
778 progenitor cells. *Mol Ther*. 2023;31(4):1074-1087. doi:10.1016/j.ymthe.2023.02.011

779 28. Papapetrou EP, Schambach A. Gene Insertion Into Genomic Safe Harbors for
780 Human Gene Therapy. *Mol Ther J Am Soc Gene Ther*. 2016;24(4):678-684.
781 doi:10.1038/mt.2016.38

782 29. Gomez-Ospina N, Scharenberg SG, Mostrel N, et al. Human genome-edited
783 hematopoietic stem cells phenotypically correct Mucopolysaccharidosis type I. *Nat*
784 *Commun*. 2019;10(1):4045. doi:10.1038/s41467-019-11962-8

785 30. Fang J, Yi S, Simmons A, et al. An antibody delivery system for regulated
786 expression of therapeutic levels of monoclonal antibodies in vivo. *Mol Ther J Am*
787 *Soc Gene Ther*. 2007;15(6):1153-1159. doi:10.1038/sj.mt.6300142

788 31. Reinhardt A, Kagawa H, Woltjen K. N-Terminal Amino Acids Determine KLF4
789 Protein Stability in 2A Peptide-Linked Polycistronic Reprogramming Constructs.
790 *Stem Cell Rep*. 2020;14(3):520-527. doi:10.1016/j.stemcr.2020.01.014

791 32. Selvaraj S, Feist WN, Viel S, et al. High-efficiency transgene integration by
792 homology-directed repair in human primary cells using DNA-PKcs inhibition. *Nat*
793 *Biotechnol*. Published online August 3, 2023:1-14. doi:10.1038/s41587-023-01888-4

794 33. Wimberger S, Akrap N, Firth M, et al. Simultaneous inhibition of DNA-PK and PolΘ
795 improves integration efficiency and precision of genome editing. Published online
796 December 15, 2022:2022.12.15.520396. doi:10.1101/2022.12.15.520396

797 34. Schiroli G, Conti A, Ferrari S, et al. Precise Gene Editing Preserves Hematopoietic
798 Stem Cell Function following Transient p53-Mediated DNA Damage Response. *Cell*
799 *Stem Cell*. 2019;24(4):551-565.e8. doi:10.1016/j.stem.2019.02.019

800 35. Ferrari S, Jacob A, Cesana D, et al. Choice of template delivery mitigates the
801 genotoxic risk and adverse impact of editing in human hematopoietic stem cells. *Cell*
802 *Stem Cell*. 2022;29(10):1428-1444.e9. doi:10.1016/j.stem.2022.09.001

803 36. Kanter J, Walters MC, Krishnamurti L, et al. Biologic and Clinical Efficacy of
804 LentiGlobin for Sickle Cell Disease. *N Engl J Med*. 2022;386(7):617-628.
805 doi:10.1056/NEJMoa2117175

806 37. George LA, Sullivan SK, Giermasz A, et al. Hemophilia B Gene Therapy with a
807 High-Specific-Activity Factor IX Variant. *N Engl J Med*. 2017;377(23):2215-2227.
808 doi:10.1056/NEJMoa1708538

809 38. Nişli G, Kavakli K, Aydinok Y, Oztop S, Cetingül N. Serum erythropoietin levels in
810 patients with beta thalassemia major and intermedia. *Pediatr Hematol Oncol*.
811 1997;14(2):161-167. doi:10.3109/08880019709030902

812 39. Halldorsson BV, Eggertsson HP, Moore KHS, et al. The sequences of 150,119
813 genomes in the UK Biobank. *Nature*. 2022;607(7920):732-740. doi:10.1038/s41586-
814 022-04965-x

815 40. Gudbjartsson DF, Helgason H, Gudjonsson SA, et al. Large-scale whole-genome
816 sequencing of the Icelandic population. *Nat Genet*. 2015;47(5):435-444.
817 doi:10.1038/ng.3247

818 41. Khan IF, Hirata RK, Russell DW. AAV-mediated gene targeting methods for human
819 cells. *Nat Protoc*. 2011;6(4):482-501. doi:10.1038/nprot.2011.301

820 42. Aurnhammer C, Haase M, Muether N, et al. Universal real-time PCR for the
821 detection and quantification of adeno-associated virus serotype 2-derived inverted
822 terminal repeat sequences. *Hum Gene Ther Methods*. 2012;23(1):18-28.
823 doi:10.1089/hgtb.2011.034

824 43. Bak RO, Porteus MH. CRISPR-Mediated Integration of Large Gene Cassettes Using
825 AAV Donor Vectors. *Cell Rep*. 2017;20(3):750-756.
826 doi:10.1016/j.celrep.2017.06.064

827 44. Bak RO, Dever DP, Porteus MH. CRISPR/Cas9 genome editing in human
828 hematopoietic stem cells. *Nat Protoc*. 2018;13(2):358-376.
829 doi:10.1038/nprot.2017.143

830 45. Charlesworth CT, Camarena J, Cromer MK, et al. Priming Human Repopulating
831 Hematopoietic Stem and Progenitor Cells for Cas9/sgRNA Gene Targeting. *Mol*
832 *Ther Nucleic Acids*. 2018;12:89-104. doi:10.1016/j.omtn.2018.04.017

833 46. Cromer MK, Vaidyanathan S, Ryan DE, et al. Global Transcriptional Response to
834 CRISPR/Cas9-AAV6-Based Genome Editing in CD34+ Hematopoietic Stem and
835 Progenitor Cells. *Mol Ther*. 2018;26(10):2431-2442.
836 doi:10.1016/j.ymthe.2018.06.002

837 47. Hu J, Liu J, Xue F, et al. Isolation and functional characterization of human
838 erythroblasts at distinct stages: implications for understanding of normal and
839 disordered erythropoiesis in vivo. *Blood*. 2013;121(16):3246-3253.
840 doi:10.1182/blood-2013-01-476390

841 48. Cradick TJ, Qiu P, Lee CM, Fine EJ, Bao G. COSMID: A Web-based Tool for
842 Identifying and Validating CRISPR/Cas Off-target Sites. *Mol Ther Nucleic Acids*.
843 2014;3(12):e214. doi:10.1038/mtna.2014.64

844 49. Clement K, Rees H, Canver MC, et al. CRISPResso2 provides accurate and rapid
845 genome editing sequence analysis. *Nat Biotechnol*. 2019;37(3):224-226.
846 doi:10.1038/s41587-019-0032-3

847

Figure 1

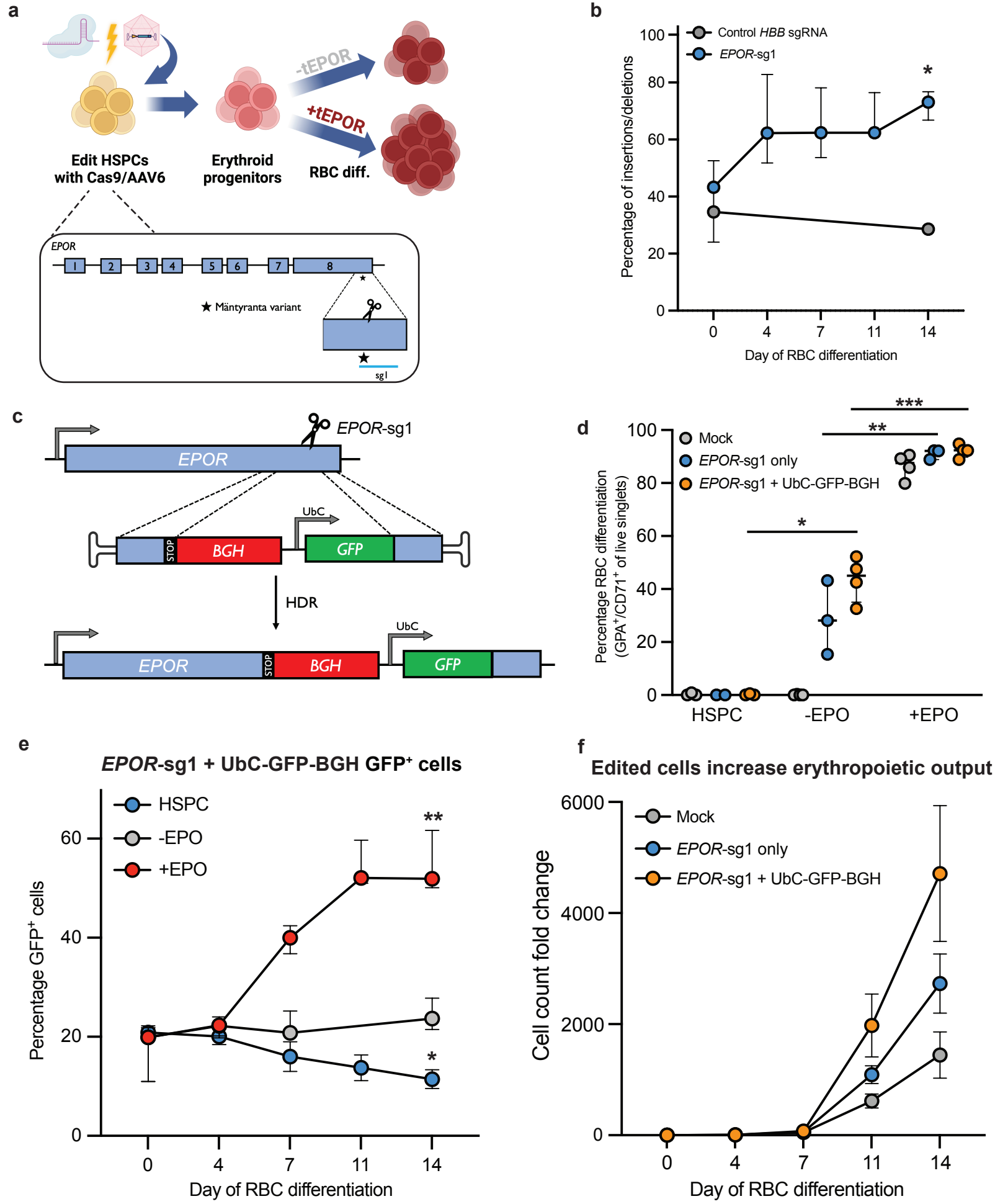
a
Edit HSPCs with Cas9/AAV6
Erythroid progenitors
-tEPOR
+tEPOR
RBC diff.
EPOR
1
2
3
4
5
6
7
8
Mäntyranta variant
sgI
b
Control HBB sgRNA
EPOR-sg1
Percentage of insertions/deletions
Day of RBC differentiation
c
EPOR-sg1
EPOR
UbC
STOP
BGH
GFP
HDR
d
Mock
EPOR-sg1 only
EPOR-sg1 + UbC-GFP-BGH
Percentage RBC differentiation (GPA+/CD71+ of live singlets)
HSPC
-EPO
+EPO
e
EPOR-sg1 + UbC-GFP-BGH GFP+ cells
HSPC
-EPO
+EPO
Percentage GFP+ cells
Day of RBC differentiation
f
Edited cells increase erythropoietic output
Mock
EPOR-sg1 only
EPOR-sg1 + UbC-GFP-BGH
Cell count fold change
Day of RBC differentiation

Figure 1: Cas9-guided *EPOR* truncation in HSPCs enhances erythroid proliferation. **a.** Schematic of HSPC editing and model of tEPOR effect. Representation of *EPOR* gene and location of the candidate sgRNA (*EPOR*-sg1) indicated by a line. Location of c.1316G>A mutation is denoted by the star. **b.** Frequency of indels created by sg1 in primary human $CD34^+$ HSPCs over the course of erythroid differentiation compared to control *HBB* sgRNA. Points represent median ± interquartile range. Values represent biologically independent HSPC donors: N=5 for *EPOR*-sg1, N=1 for control *HBB* sgRNA. *P=0.0016 of day 1 vs. day 14 by unpaired two-tailed *t*-test. **c.** Genome editing strategy when using an AAV6 DNA repair template to introduce the *EPOR* c.1316G>A mutation followed by a BGH-polyA region and UbC-driven GFP reporter. **d.** Percentage of $GPA^+/CD71^+$ of live single cells on day 14 of differentiation. Bars represent median ± interquartile range. Values represent biologically independent HSPC donors: N=2-3 for HSPC, N=3-4 for -EPO and +EPO conditions. *P=0.0016 of -EPO vs. HSPC conditions; **P=0.003 and ***P=0.0001 of -EPO vs. +EPO conditions by unpaired two-tailed *t*-test. **e.** Percentage of GFP^+ cells of live single cells maintained in RBC media +/- EPO or HSPC media as determined by flow cytometry. Points represent median ± interquartile range. Values represent biologically independent HSPC donors N=2 for HSPC condition and N=3-4 for -EPO and +EPO conditions. *P=0.04, **P=0.0006 of day 0 vs. day 14 by unpaired two-tailed *t*-test. **f.** Fold change in cell count throughout RBC differentiation (e.g., if at day 0 starting cell numbers were 1E5 cells total, therefore a fold count change of 1000 would yield a total cell number of 1E8 at day 14). Points represent mean ± SEM. Values represent biologically independent HSPC donors N=3 for Mock and *EPOR*-sg1 + BGH and N=2 for *EPOR*-sg1.

Figure 2

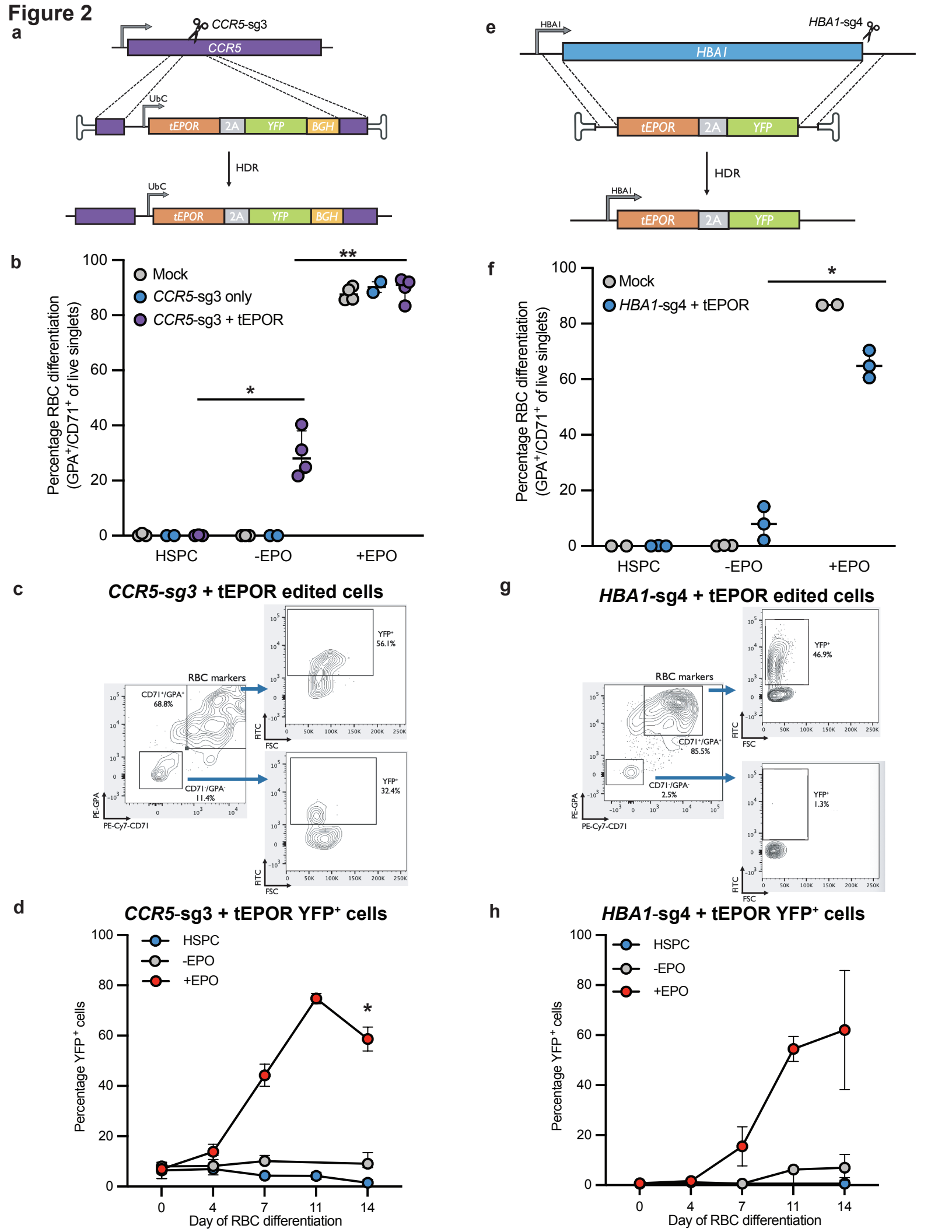
a
CCR5-sg3
CCR5
UbC
tEPOR
2A
YFP
BGH
HDR
UbC
tEPOR
2A
YFP
BGH
e
HBA1
HBA1-sg4
HBA1
tEPOR
2A
YFP
HDR
HBA1
tEPOR
2A
YFP
b
Mock
CCR5-sg3 only
CCR5-sg3 + tEPOR
Percentage RBC differentiation (GPA+/CD71+ of live singlets)
100
80
60
40
20
0
*
**
HSPC
-EPO
+EPO
f
Mock
HBA1-sg4 + tEPOR
Percentage RBC differentiation (GPA+/CD71+ of live singlets)
100
80
60
40
20
0
*
HSPC
-EPO
+EPO
c
CCR5-sg3 + tEPOR edited cells
RBC markers
CD71+/GPA+
68.8%
CD71-/GPA-
11.4%
PE-GPA
PE-Cy7-CD71
YFP+
56.1%
YFP+
32.4%
FITC
FSC
g
HBA1-sg4 + tEPOR edited cells
RBC markers
CD71+/GPA+
85.5%
CD71-/GPA-
2.5%
PE-GPA
PE-Cy7-CD71
YFP+
46.9%
YFP+
1.3%
FITC
FSC
d
CCR5-sg3 + tEPOR YFP+ cells
HSPC
-EPO
+EPO
Percentage YFP+ cells
100
80
60
40
20
0
*
0
4
7
11
14
Day of RBC differentiation
h
HBA1-sg4 + tEPOR YFP+ cells
HSPC
-EPO
+EPO
Percentage YFP+ cells
100
80
60
40
20
0
0
4
7
11
14
Day of RBC differentiation

Figure 2: Integration of *tEPOR* cDNA demonstrates an erythroid-specific proliferative effect.

a. Genome editing strategy to introduce *tEPOR*-T2A-YFP-BGH-polyA cDNA at the *CCR5* locus with expression driven by a ubiquitous UbC promoter. **b.** Percentage of $GPA^+/CD71^+$ of live single cells on day 14 of differentiation following introduction of *tEPOR* at *CCR5* locus. Bars represent median ± interquartile range. Values represent biologically independent HSPC donors: N=2-3 for HSPC condition, N=2-4 for -EPO and +EPO conditions. *P=0.0018 of -EPO vs. HSPC conditions; **P<0.0001 of -EPO vs. +EPO conditions by unpaired two-tailed *t*-test. **c.** Representative flow cytometry plots of one donor of *CCR5*-sg3 + tEPOR-edited HSPCs on day 14 of RBC differentiation in the +EPO condition. **d.** Percentage of YFP^+ cells of live single cells as determined by flow cytometry. Points represent mean ± SEM. Values represent biologically independent HSPC donors: N=2 for HSPC condition, N=3 for -EPO condition, N=3-4 for +EPO condition. *P = 0.0003 of day 0 vs. day 14 by unpaired two-tailed *t*-test. **e.** Genome editing strategy to introduce *tEPOR*-T2A-YFP cDNA at the *HBA1* locus by whole gene replacement to place integration cassette under regulation of the endogenous *HBA1* promoter. **f.** Percentage of $GPA^+/CD71^+$ of live single cells on day 14 of differentiation following introduction of *tEPOR* cDNA at the *HBA1* locus. Bars represent median ± 95% confidence interval. Values represent biologically independent HSPC donors: N=2 for HSPC condition, N=2-3 for -EPO and +EPO condition. *P=0.0002 of -EPO to +EPO condition by unpaired two-tailed *t*-test. **g.** Representative flow cytometry plots of one donor of *HBA1*-sg4 + tEPOR-edited HSPCs on day 11 of RBC differentiation in the +EPO condition. **h.** Percentage of YFP^+ cells of live single cells as determined by flow cytometry. Points represent mean ±

SEM. Values represent biologically independent HSPC donors: N=2 for HSPC condition, N=3 for -EPO and +EPO condition.

Figure 3

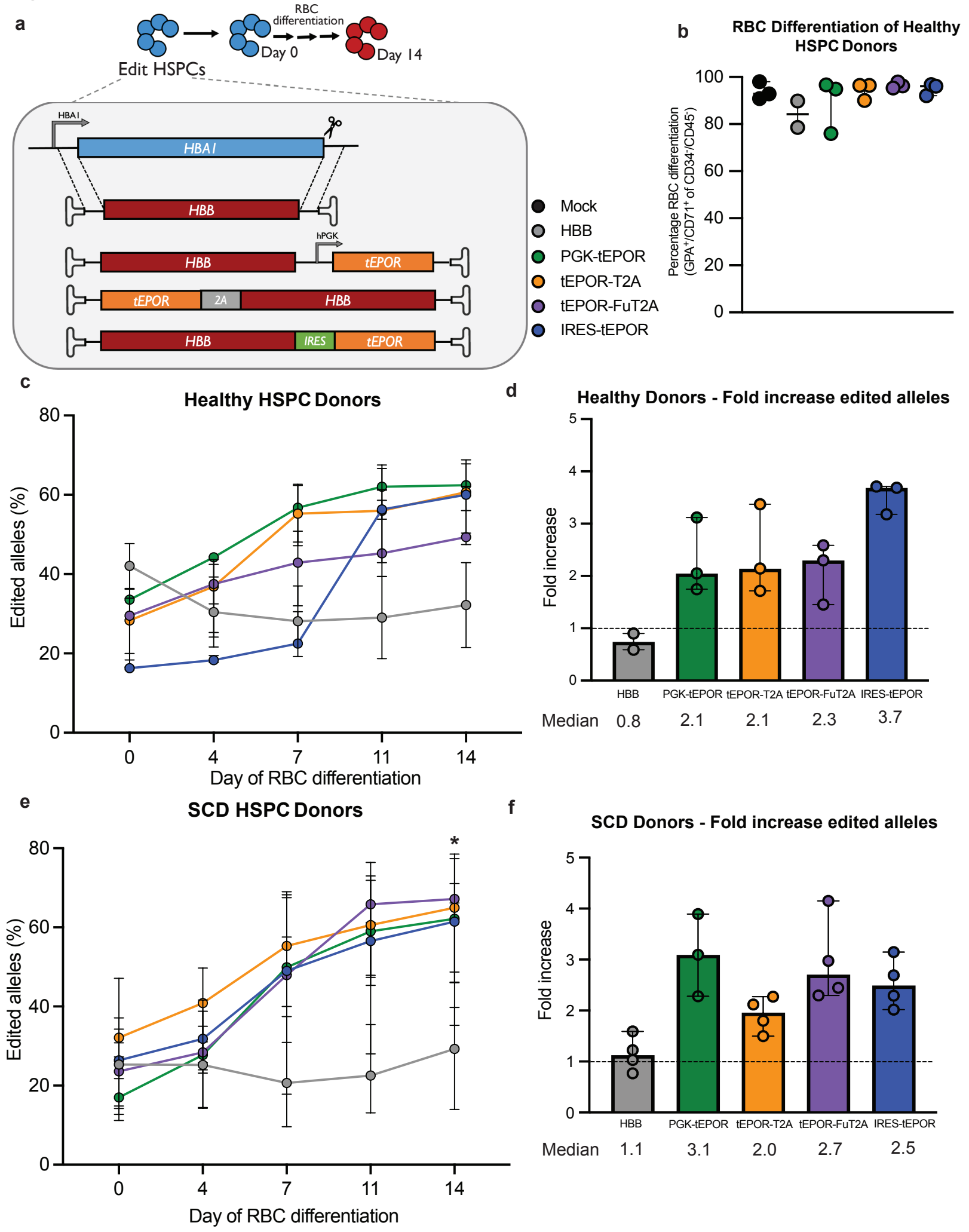
a
Edit HSPCs
RBC differentiation
Day 0
Day 14
HBA1
HBA1
HBB
hPGK
HBB
tEPOR
tEPOR
2A
HBB
HBB
IRES
tEPOR
Mock
HBB
PGK-tEPOR
tEPOR-T2A
tEPOR-FuT2A
IRES-tEPOR
b
RBC Differentiation of Healthy HSPC Donors
Percentage RBC differentiation (GPA+/CD71+ of CD34+/CD45-)
100
80
60
40
20
0
c
Healthy HSPC Donors
Edited alleles (%)
80
60
40
20
0
0
4
7
11
14
Day of RBC differentiation
d
Healthy Donors - Fold increase edited alleles
Fold increase
5
4
3
2
1
0
HBB
PGK-tEPOR
tEPOR-T2A
tEPOR-FuT2A
IRES-tEPOR
Median
0.8
2.1
2.1
2.3
3.7
e
SCD HSPC Donors
Edited alleles (%)
80
60
40
20
0
*
0
4
7
11
14
Day of RBC differentiation
f
SCD Donors - Fold increase edited alleles
Fold increase
5
4
3
2
1
0
HBB
PGK-tEPOR
tEPOR-T2A
tEPOR-FuT2A
IRES-tEPOR
Median
1.1
3.1
2.0
2.7
2.5

Figure 3: Therapeutic editing frequencies are achieved using bicistronic *HBB-tEPOR* cassette.

a. Design of *HBB* (control) and *HBB-tEPOR* (bicistronic) AAV6 donor cassettes targeted to the *HBA1* locus by whole gene replacement. **b.** Percentage of $GPA^+/CD71^+$ of $CD34^-/CD45^-$ cells on day 14 as determined by flow cytometry. Points shown as median ± 95% confidence interval. Values represent biologically independent HSPC donors: N=2 for HBB, N=3 for all other vectors. **c.** Percentage of edited alleles for control (*HBB*) and bicistronic *HBB-tEPOR* in cord-blood derived $CD34^+$ cells over the course of RBC differentiation. Points shown as median ± 95% confidence interval. Values represent biologically independent HSPC donors: N=2 for HBB, N=3 for all other vectors. *P=0.003 for PGK-*tEPOR*, P=0.0055 for T2A-*tEPOR*, P=0.0259 for Fu2A-*tEPOR*, and P=0.0003 for IRES-*tEPOR* (day 0 vs. day 14) by unpaired two-tailed *t*-test. **d.** Fold change in edited alleles from beginning (day 0) to end (day 14) of RBC differentiation. Bars represent median ± 95% confidence interval. **e.** Percentage of edited alleles for control (*HBB*) and bicistronic *HBB-tEPOR* vectors in sickle cell disease patient cells over the course of RBC differentiation. Points shown as median ± 95% confidence interval. Values represent biologically independent HSPC donors: N=3 for PGK-*tEPOR*, N=4 for all other vectors. *P=0.0061 for PGK-*tEPOR*, P=0.011 for T2A-*tEPOR*, P=0.0016 for Fu2A-*tEPOR*, P=0.0153 for IRES-*tEPOR* (day 0 vs. day 14) by unpaired two-tailed *t*-test. **f.** Fold change in edited alleles from beginning (day 0) to end (day 14) of RBC differentiation. Bars represent median ± standard deviation.

Figure 4

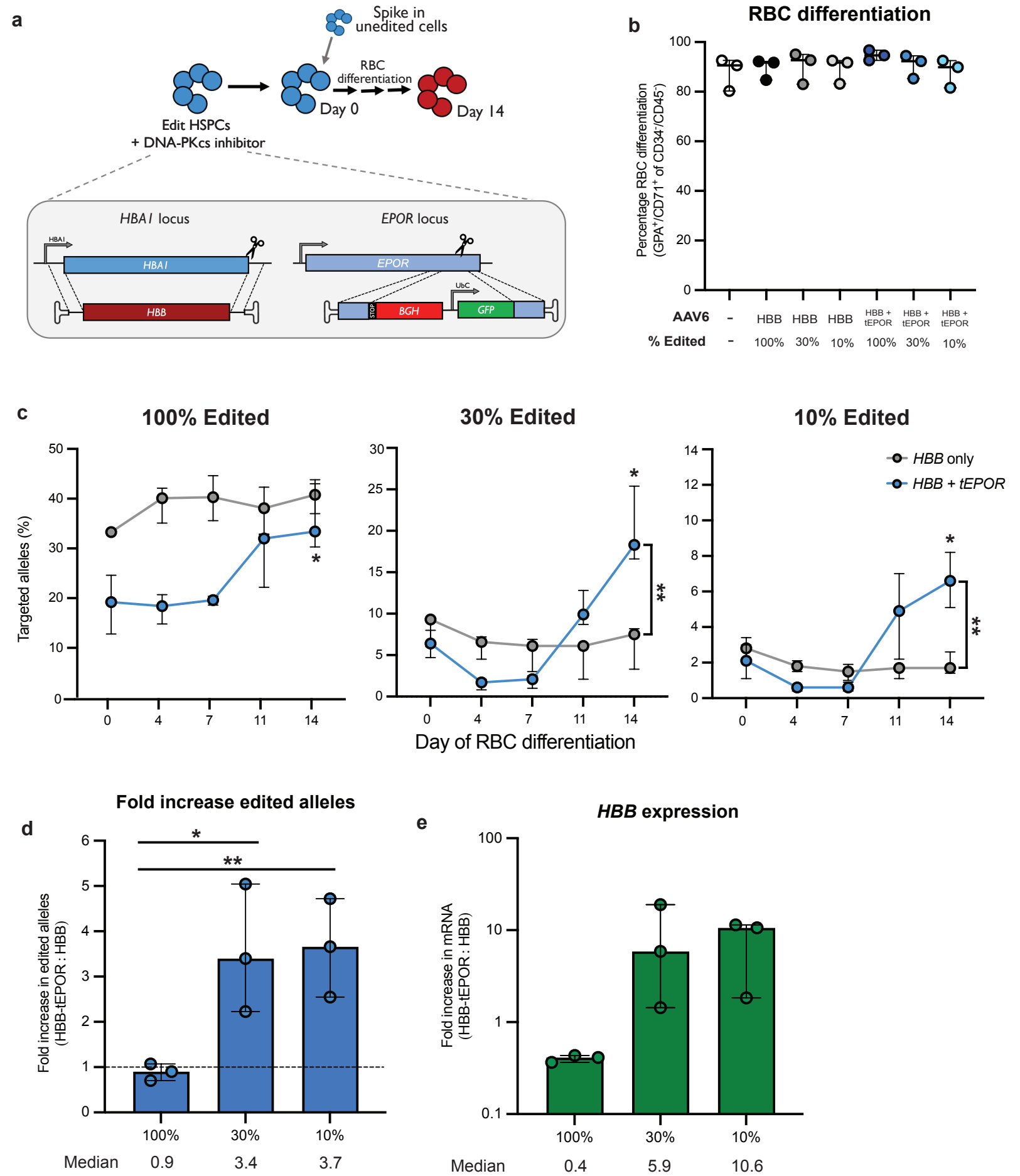
a
Spike in unedited cells
RBC differentiation
Day 0
Day 14
Edit HSPCs
+ DNA-PKcs inhibitor
HBA1 locus
EPOR locus
HBA1
HBB
EPOR
UbC
STOP
BGH
GFP
b
RBC differentiation
Percentage RBC differentiation (GPA+/CD71+ of CD34-/CD45-)
AAV6
% Edited
HBB
HBB + tEPOR
100%
30%
10%
c
100% Edited
30% Edited
10% Edited
Targeted alleles (%)
Day of RBC differentiation
HBB only
HBB + tEPOR
d
Fold increase edited alleles
Fold increase in edited alleles (HBB-tEPOR : HBB)
Median
0.9
3.4
3.7
e
HBB expression
Fold increase in mRNA (HBB-tEPOR : HBB)
Median
0.4
5.9
10.6

Figure 4: Multiplexed editing of *EPOR* and *HBA1* leads to robust increase in *HBB* mRNA within editing HSPCs.

a. Schematic of multiplexed editing strategy with spike-in of unedited cells at start of erythroid differentiation to model HSPC transplantation. **b.** Percentage of $GPA^+/CD71^+$ of $CD34^-/CD45^-$ cells on day 14 of RBC differentiation as determined by flow cytometry. Points shown as median ± interquartile range. N=3 biologically independent HSPC donors. **c.** Percentage of edited alleles at *HBA1* in all multiplexed editing/spike-in conditions throughout RBC differentiation. Points shown as median ± 95% confidence interval. N=3 biologically independent HSPC donors. *P=0.0332 for *HBB*+*tEPOR* 100%, P=0.0086 for *HBB*+*tEPOR* 30%, P=0.0122 for *HBB*+*tEPOR* 10% (day 0 vs. day 14) by unpaired two-tailed *t*-test. **P=0.0113 for *HBB* versus *HBB*+*tEPOR* 30% at day 14 and P=0.008 for HBB versus *HBB*+*tEPOR* 10% at day 14 by unpaired two-tailed *t*-test. **d.** Fold increase in edited alleles on day 14 of differentiation of multiplexed conditions versus *HBB* only. Bars represent median ± 95% confidence interval. *P=0.0315 and **P=0.0123 by unpaired two-tailed *t*-test. **e.** mRNA expression of integrated *HBB* at *HBA1* locus normalized to *HBB* expression from mock. *GPA* mRNA expression was used as a reference. N=3 biologically independent HSPC donors. Bars represent median ± 95% confidence interval.